ACADEMIC PRESS

Available online at www.sciencedirect.com

SCIENCE DIRECT®

DEVELOPMENTAL BIOLOGY

Developmental Biology 264 (2003) 391–406

www.elsevier.com/locate/ydbio

Zic2 is required for neural crest formation and hindbrain patterning during mouse development

Paul Elms,[a] Pam Siggers,[b] Diane Napper,[a] Andy Greenfield,[b] and Ruth Arkell[a,*]

[a] *Laboratory of Early Development, Mammalian Genetics Unit, MRC, Harwell, Oxfordshire, OX11 ORD, UK*
[b] *Laboratory of Sexual Development, Mammalian Genetics Unit, MRC, Harwell, Oxfordshire, OX11, ORD, UK*

Received for publication 19 May 2003, revised 8 September 2003, accepted 8 September 2003

Abstract

The *Zic* genes are the vertebrate homologues of the *Drosophila* pair rule gene *odd-paired*. It has been proposed that *Zic* genes play several roles during neural development including mediolateral segmentation of the neural plate, neural crest induction, and inhibition of neurogenesis. Initially during mouse neural development *Zic2* is expressed throughout the neural plate while later on expression in the neurectoderm becomes restricted to the lateral region of the neural plate. A hypomorphic allele of *Zic2* has demonstrated that in the mouse *Zic2* is required for the timing of neurulation. We have isolated a new allele of *Zic2* that behaves as a loss of function allele. Analysis of this mutant reveals two further functions for *Zic2* during early neural development. Mutation of *Zic2* results in a delay of neural crest production and a decrease in the number of neural crest cells that are produced. These defects are independent of mediolateral segmentation of the neurectoderm and of dorsal neurectoderm proliferation, both of which occur normally in the mutant embryos. Additionally *Zic2* is required during hindbrain patterning for the normal development of rhombomeres 3 and 5. This work provides the first genetic evidence that the *Zic* genes are involved in neural crest production and the first demonstration that *Zic2* functions during hindbrain patterning.

Keywords: Neural crest; Hindbrain; ENU; *Zic*; Wnt6

Introduction

The neural crest is a transitory population of cells that arises at the boundary of the neural and nonneural ectoderm (Chan and Tam, 1988; Le Douarin and Kalcheim, 1999). During neurulation the crest cells undergo an epithelial to mesenchymal transition, detach from the margin of the neural plate, and migrate away from the neurectoderm along defined pathways. Ultimately the neural crest will form a wide variety of cell types that include the pigment-producing melanoblasts, and neurons and glial cells of the peripheral nervous system (Kaufman and Bard, 1999). In recent years many genes have been proposed to play a role in neural crest formation, based predominantly on the basis of in vivo or in vitro overexpression studies (for review, see Knecht and Bronner-Fraser, 2002, and Aybar and Mayor, 2002). To determine whether these genes are required for endogenous crest formation loss of function studies are necessary. The ability to perform genetic analysis in the mouse means that it is an ideal organism in which to study neural crest formation. Additionally, classical genetics has shown that in some cases visible phenotypes are associated with defects in crest production. This allows the use of an unbiased, phenotype-driven approach to the identification of genes that are required for mammalian neural crest formation.

The neural crest gives rise to all of the pigment-producing cells in the mouse skin and coat. As a result, small defects in crest generation or migration may be seen as white regions among an otherwise coloured mouse coat. Classical mouse genetics has identified several mouse mutants that affect crest production including splotch (*Pax3*) (Russell, 1947), patch (*Pdgfra*) (Gruneberg and Truslove, 1960), Dominant megacolon (*Sox10*) (Lane, 1982), piebald (*Ednrb*) (Dunn, 1920), lethal spotting (*Edn3*) (Phillips,

* Corresponding author. Fax: +44-1235-84-1200.
E-mail address: r.arkell@har.mrc.ac.uk (R. Arkell).

0012-1606/$ – see front matter © 2003 Elsevier Inc. All rights reserved.
doi:10.1016/j.ydbio.2003.09.005

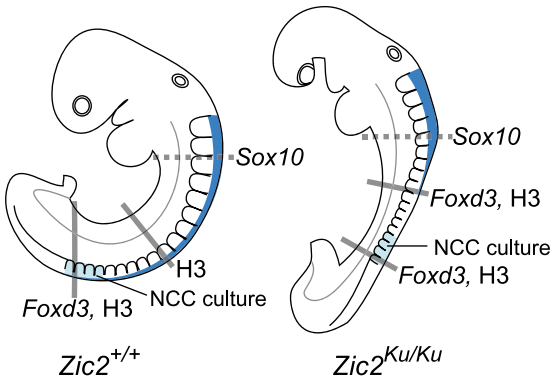

Fig. 1. Neural crest cell analysis. The diagrams represent an 18-somite stage wild-type embryo and an 18-somite stage mutant embryo with the extent of trunk neural crest production represented in dark blue. Analysis was carried out at the axial levels shown. *Sox10:* analysis of *Sox10*-positive migrating neural crest cells; *Foxd3:* analysis of *Foxd3*-positive premigratory neural crest cells; H3: analysis of anti-phospho-histone H3-positive mitotic cells; NCC culture: neural crest cell culture was carried out using neurectoderm adjacent to the four posterior-most somites.

1959), dominant spotting (*Kit*) (Little and Cloudman, 1937), and microphthalmia (*Mitf*) (Hertwig, 1942). Many of these mutations act in a semidominant manner with the phenotype being produced as a result of haploinsufficiency. Recent random mutagenesis screens for dominant mouse mutants have produced hundreds of lines of mice with visible effects on the coat (Hrabe de Angelis et al., 2000; Nolan et al., 2000). It is likely that further semidominant mutations will be found among these stocks of mutant lines and that these resources represent an opportunity to genetically dissect mammalian neural crest formation.

One family of genes that has been proposed to play a role in neural crest development is the *Zic* genes. These genes are the vertebrate homologues of the *Drosophila* gene *odd-paired (opa)* (Aruga et al., 1994). *Odd-paired* is a pair rule gene that is expressed throughout the entire pair rule domain during *Drosophila* embryogenesis. Studies of *opa* mutants suggest that *opa* is a transcription factor that interacts with other, spatially restricted, transcription factors to specify cell fate (Benedyk et al., 1994). All of the *opa*-related genes so far isolated contain five C2H2 zinc finger domains that have high sequence homology to the *ci/Gli* genes, and it has been shown that Zic and Gli proteins can bind to one another in vitro (Koyabu et al., 2001). The vertebrate genes were named *Zic* genes because they were originally isolated from cerebellum (zinc finger of the cerebellum), and in postbirth stages, this appears to be their predominant site of

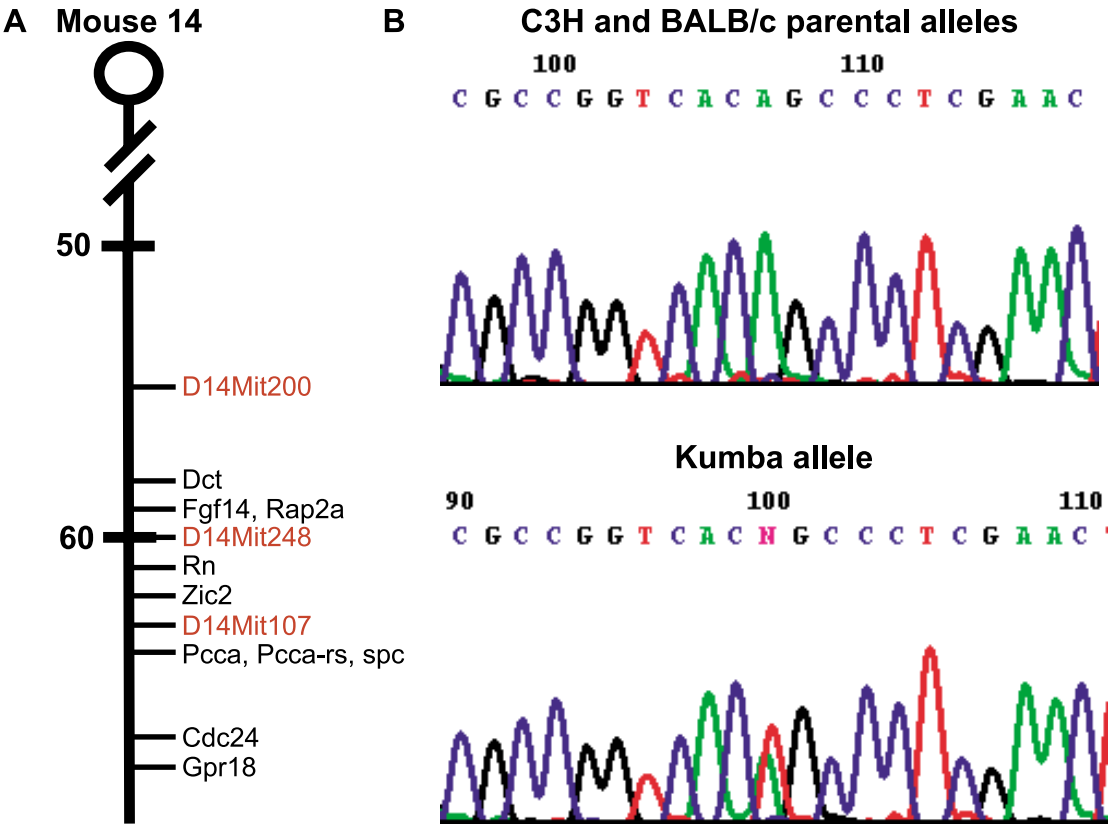

Fig. 2. *Zic2* is mutated in Kumba mutants. (A) All affected progeny were nonrecombinant at D14Mit248 and D14 Mit107, but not at D14Mit200, localising the mutation distal of D14Mit200. All of the genes known to map to this region at the time of cloning are shown on the map. (B) A sequence trace from either of the parental alleles (C3H/HeH and BALB/c) showing an "A" at the 11th nucleotide and a sequence trace from a Ku/+ mouse showing an "A" or a "T" at this position. This A1350T mutation causes a Cys370Ser substitution.

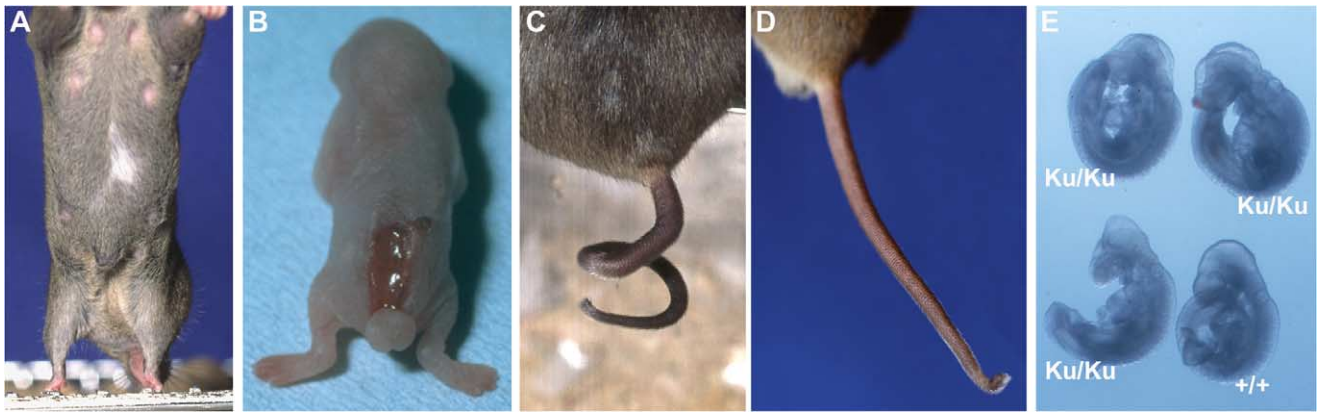

Fig. 3. The Kumba mutant phenotype. The range of $Zic2^{Ku/+}$ phenotypes (A–D) are shown. (A) Ventral spot, (B) Spina bifida and curled tail, (C) Curled tail, or (D) Distal tail kink. (E) Three $Zic2^{Ku/Ku}$ 9.5 dpc embryos are shown alongside a wild-type littermate. The homozygotes can be distinguished by an open cranial neural tube, delayed posterior neuropore closure, and haemotomas on the forebrain.

expression. In mice, there are three *Zic* genes (*Zic 1, 2,* and *3*) that have high homology throughout the entire zinc finger domain. Two further genes (*Zic4* and *Opr*) show high homology with all of the *Zic* genes between Zinc fingers 2 and 5, but have a divergent zinc finger 1 (Aruga et al., 1996a,b; Furushima et al., 2000).

The role of the vertebrate *Zic* genes in neural development has been most intensively studied using overexpression assays in *Xenopus*. Each of the *Zic* genes tested in these assays (*Zic1–3* and *Zic5*) is able to induce the expression of neural crest markers in the absence of mesoderm induction (Brewster et al., 1998; Mizuseki et al., 1998; Nakata et al., 1997, 2000). When *Zic1, Zic2,* or *Zic3* is overexpressed, the crest induction occurs alongside the induction of anterior neural markers (cement gland and forebrain); additionally each of these genes is able to induce the expression of itself and of all of the other *Zic* genes (Nakata et al., 2000). This has led to the proposal that these genes act at an early stage of crest development when the neural plate is first specified and still has anterior character. The *Zic* genes may segment the ectoderm into broad domains that include neural plate border. Another member of the *Xenopus Zic* gene family, *Zic5* (which is homologous to mouse *Opr*), is expressed in a more neural crest-specific manner in *Xenopus* embryos. Overexpression of *Zic5* causes ectopic expression of neural crest markers, but not of anterior neural markers. Instead *En2* (which marks the midbrain/hindbrain junction) is induced (Nakata et al., 2000). The induction of more posterior neural markers, along with the more restricted pattern of expression, suggests that *Zic5* may act later than the other *Zic* genes to specify neural crest cell fates.

In the mouse, mutant alleles exist for *Zic1, 2,* and *3*. A targeted null allele of *Zic1* shows no embryonic phenotype (Aruga et al., 1998). A hypomorphic allele of *Zic2* was constructed by gene targeting and embryos homozygous for this allele die perinatally and exhibit defects in neurulation and forebrain development. No primary defect in neural crest generation or hindbrain development was reported in this study (Nagai et al., 2000). *Zic3* is deleted in the classical mouse mutant Bent tail (*Bn*) (Carrel et al., 2000; Klootwijk et al., 2000), and a second null allele has been generated by gene targeting (Purandare et al., 2002). An effect on neural development has not been demonstrated in either of the *Zic3* alleles. Here we show that the Kumba (*Ku*) mouse mutant isolated from a mutagenesis experiment (Nolan et al., 2000) is a new allele of *Zic2*. The ENU-induced point mutation is in the 4th zinc finger and is predicted to abolish the function of the zinc finger domain. A small proportion of the mice that are heterozygous for this mutation exhibit a neurulation defect and some heterozygotes have a white spot on their underbelly, suggesting a role in neural crest development. Analysis of mice that are homozygous for this mutation demonstrates that, like the targeted allele, they have defects in neurulation and forebrain development. However, these homozygotes die at midgestation and exhibit defects not identified in the hypomorphic allele. Specifically they have a defect in production of the neural crest and display defective hindbrain patterning. This represents the first genetic evidence that *Zic2* is involved in either of these processes.

Materials and methods

Mouse husbandry

The $Zic2^{Ku}$ allele was maintained by continuous backcross to C3H/HeH inbred mice. To generate embryos for analysis C3H/HeH congenic males and females (from the 10th backcross generation and beyond) that were heterozygous for the $Zic2^{Ku}$ allele were selected for intercross matings. Mice were maintained in a light cycle of 12-h light: 12-h dark, the midpoint of the dark cycle being 1 AM. One PM on the day of appearance of the vaginal plug is designated 0.5 dpc. To genotype mice for the presence of the Kumba mutation DNA was prepared

from tail tissue as described in Arkell et al. (2001). PCR was performed using an allelic discrimination assay designed using ABI Prism Primer Express and the reactions carried out using an ABI 7000 Real-Time PCR machine according to the manufacturer's instructions.

Positional candidate cloning

Genomic DNA was isolated from biopsy of mouse tail tissue using the Nucleon BACC2 DNA Kit. To refine the location of the mutation on chromosome 14, 50 ng of DNA was amplified in a reaction volume of 20 μl using a set of simple sequence length polymorphism (SSLP) markers from mouse chromosome 14: D14Mit5, D14Mit13, D14Mit37, D14Mit123, D14Mit39, D14Mit34, D14Mit239, D14Mit70, D14Mit170, D14Mit200, D14Mit248, and D14Mit107. PCR products were resolved by SSCP analysis with 8% nondenaturing PAGE and silver staining (Denny and Brown, 2000). To assess *Zic2* candidature, the *Zic2* coding sequence was amplified from genomic DNA and the PCR products resolved using the same protocols described for the SSLP analysis. For direct sequencing of PCR products the reactions were purified using QIAquick columns (Qiagen). All sequencing was performed using an ABI377 sequencer and the ABI Prism Big Dye Cycle Sequence Ready Reaction Kit (PE Biosystems). Sequences were analysed using Jellyfish (LabVelocity).

cDNA clones

For whole-mount in situ hybridisation (WMISH) to *Zic2*, a cDNA probe corresponding to bases 273–1010 of mouse *Zic2* (accession no. NM_009574) was amplified and cloned into pGEM-Teasy (Promega). An antisense riboprobe was generated to this clone by *Sal*I digest and transcription with T7 polymerase. *Foxd3*, *Hoxa2*, and *Sox10* probes were all generated from I.M.A.G.E Consortium [LLNL] cDNA Clones (Lennon et al., 1996). The details of each clone are as follows. *Foxd3:* I.M.A.G.E ID 418507, accession no. AI43048, digested with *Hin*dIII and transcribed with T7 polymerase. *Hoxa2:* I.M.A.G.E ID 333548, accession no. AI324701, digested with *Hind*III and transcribed with T7 polymerase. *Sox10:* I.M.A.G.E ID 4164053, accession no. BF301006, digested with *Sal*I and transcribed with T7 polymerase. A *Wnt6* antisense probe was generated by direct transcription of a PCR product corresponding to 440 bp of *Wnt6* exon 4 (bases 653–1092 of NM_009526.1) using a 3′ primer incorporating the T7 RNA polymerase promoter. The following probes for WMISH were as described previously: *Tcfap2a (AP-2;* Mitchell et al., 1991), Follistatin (Albano et al., 1994), *Krox-20* (Wilkinson et al., 1989), and *Msx1* (Hill et al., 1989), *Shh* (Echelard et al., 1993), BMP7 (Arkell and Beddington, 1997).

Embryo recovery and WMISH

All embryos were dissected in PBS with 10% newborn calf serum. Embryos for WMISH and immunohistochemistry were dissected from maternal tissue and Reichert's membrane removed. The amnion was removed and holes made in the embryos in regions likely to trap probe. Embryos were transferred to 4% paraformaldehyde in PBS and yolk sacs were transferred to lysis solution (TE, pH 7.5, and 0.1% Tween 20: polyoxyetylene sorbitan monolaurate; Sigma) and DNA prepared for PCR as described in Arkell et al. (2001). Embryos were genotyped using an allelic discrimination assay as described above. WMISH was carried out according to Wilkinson (1992), using the hybridisation conditions of Rosen and Beddington (1993). After completion of the in situ procedure, embryos were destained in PBT (PBS with 0.1% Tween 20) for 48 h and postfixed in 4% paraformaldehyde in PBS for 1 h at room temperature. Embryos were either photographed under PBS on a 0.5% agarose in PBS petri dish, or processed for photography through a glycerol series (50%, 80%, 100%) and photographed in 100% glycerol on a glass slide. At this stage the surface ectoderm, endoderm, and paraxial and lateral mesoderm were removed from some embryos using tungsten needles. These embryos were placed on a glass microscope slide, under a coverslip, and the neurectoderm photographed. Before embedding for cryosectioning, embryos were returned to PBS and again postfixed in 4% paraformaldehyde in PBS. The specimens were placed into OCT cyroembedding solution (BDH) and flash-frozen in liquid nitrogen; 18-μm sections were cut using a Microm cryostat. Detection of anti-phosphohistone H3 antibody (Upstate Biotechnology) was performed on cryostat sections of paraformaldehyde (4%) fixed tissue according to the manufacturer's protocols. The primary antibody was diluted 1:200 and detected with HRP-conjugated secondary antibody (Vector Labs) diluted 1:100. Peroxidase was detected by incubation in 0.5 mg/ml DAB and 0.01% H_2O_2 in PBS for 10 min at room temperature.

Cell counting

The strategies used for cell counting are shown in Fig. 1. Migrating neural crest cells were counted in vivo using *Sox10* expression as a molecular marker of migrating cells. Transverse sections through the trunk immediately posterior to the heart were examined under a compound microscope (Zeiss) and scored using a 40× objective. Migrating, *Sox10*-expressing cells were counted in a set of 10–12 representative sections from each embryo and scored for their migration pathway: subectodermal, ventrolateral, or ventromedial. Cells that were either still within the neurectoderm or ventral to the neural tube were not included in the analysis due to the difficulty of distinguishing individual cells in these regions. For statistical analysis the data were pooled within genotype and stage classes to compare the mean number of cells per section between mutant embryos and wild-type embryos.

To determine the number of neural crest cells that are

Table 1
Each of the $Zic2^{Ku/+}$ phenotypes is incompletely penetrant[a]

Phenotype	Observed
Ventral spot	13 (11.5%)[b]
Spina bifida	3 (2.7%)[b]
Curled tail	14 (12.4%)[b]
Tail kink	47 (41.6%)[b]
Total with any phenotype	72 (30.1%) NT
Number of heterozygotes identified by genotyping	113 (47.3%)

[a] All pups were observed daily between birth and weaning and any visible phenotypes recorded. At weaning all mice were genotyped. $n = 239$.
[b] Values are significantly different from the 50% expected, $P < 0.01$ (binomial test); NT: not tested.

formed in the neurectoderm *Foxd3* was used as a molecular marker and positive cells were scored in transverse section under a compound microscope (Zeiss) using a 40× objective. As shown in Fig. 1, in wild-type embryos the number of *Foxd3*-positive cells in the dorsal neurectoderm was scored in the 12 posterior-most sections that contain *Foxd3* cells. In mutant embryos counts were made at two axial levels. First, sections were analysed at an equivalent axial level to the counts made in wild-type embryos, and a second set of sections corresponding to the 12 posterior-most sections that contain *Foxd3* cells were also examined. The results were analysed as described for the *Sox10* counts.

The number of mitotically active cells was analysed by scoring cells positive for anti-phospho-histone H3 antibody. Counts of positive cells in the dorsal fifth of the neurectoderm were made from serial, transverse sections examined under a compound microscope (Zeiss) using a 40× objective. Sections were examined along the entire neuraxis and counts were made through two regions as shown in Fig. 1. One set of counts was through a set of 10–20 sections that include the anterior region of the posterior neuropore and sections immediately rostral of the neuropore. The second set of counts was through the trunk region at a level that corresponded to the posterior limit of crest production in mutant embryos. The results were analysed as described for the *Sox10* counts.

To carry out in vitro counts of neural crest cells neurectoderm from the region of the four posterior-most somites was isolated using tungsten needles after digestion in Dispase (1 U/ml, GIBCO) for 5 min at room temperature. Neurectoderm from each embryo was transferred to one well in a four-well dish coated with fibronectin (2.5 $\mu g/cm^2$; Sigma) and cultured in DMEM supplemented with 10% serum at 37°C in 6% CO_2 in humidified air for 60 h. Cultures were fixed in 4% paraformaldehyde (1 h, room temperature) and stained with haematoxylin according to standard procedures. Images of each culture were captured using a digital camera and Improvision software, the images were printed, and the number of individual neural crest cells counted.

Photography

Low-power bright-field photographs were taken in a dissecting microscope (Nikon) using tungsten film (Fuji 64T). Higher power Nomarski photographs were taken in a compound microscope (Zeiss) using tungsten film (Fuji 64T).

Results

Zic2 is mutated in Kumba mutants

The Kumba mutation was previously shown to be linked to mouse chromosome 14 (Nolan et al., 2000). Further characterisation of DNA from 30 affected individuals localised the mutation distal to D14 Mit200, as shown in Fig. 2a. Of the 10 genes mapped to this interval, the *Zic2* gene was considered a strong candidate because it is expressed in the dorsal neural tube at 9.5 dpc (Nagai et al., 1997) and because mice homozygous for a hypomorphic allele of *Zic2* are born with spina bifida (Nagai et al., 2000). We therefore examined the *Zic2* transcript in *Ku* mutants. The coding sequence of the *Zic2* gene was amplified by PCR from genomic DNA and scanned for mutations using SSCP analysis. Of the 10 amplicons analysed, one showed a difference between the affected individuals and the parental strains. All 30 affected individuals were found to contain the variant product. A further five strains of mice (Mus Castaneus, Mus Spretus, C57BL/6J, 129Sv, and 101/H) were analysed and none were found to contain the variant allele. This eliminated the possibility that the variant is a naturally occurring polymorphism. The variant product spanned exon 2 and was sequenced from 10 *Ku*-affected animals and from the parental strains. The novel SSCP product was caused by a single base pair change at nucleotide position 1350 of accession no. NM_009574 (Fig. 2b). This base pair change is an A-T transversion, the most common ENU change in mouse (Justice et al., 1999), and generates a missense mutation, causing the amino acid substitution C370S in the 4th zinc finger. The altered cysteine is a canonical residue and is required to chelate the zinc ion (Miller et al., 1985). Based on the mutation of the equivalent residue in other zinc finger proteins the substitution is predicted to abolish the function of the *Zic2* zinc finger domain (Blumberg et al., 1987; Redemann et al., 1988). Subsequent maintenance of the

Table 2
$Zic2^{Ku/Ku}$ embryos die at 13.5 dpc[a]

Stage	$Zic2^{+/+}$	$Zic2^{Ku/+}$	$Zic2^{Ku/Ku}$
9.5 dpc ($n = 107$)	26 (24.3%)	59 (55.1%)	22 (20.6%)[b]
13.5 dpc ($n = 48$)	11 (22.9%)	26 (54.2%)	11 (22.9%)[b,c]

[a] Embryos were recovered from intercross litters and genotyped.
[b] Values are not significantly different from the expected number, $P < 0.01$ (χ^2 test).
[c] The recovered embryos were dead or dying.

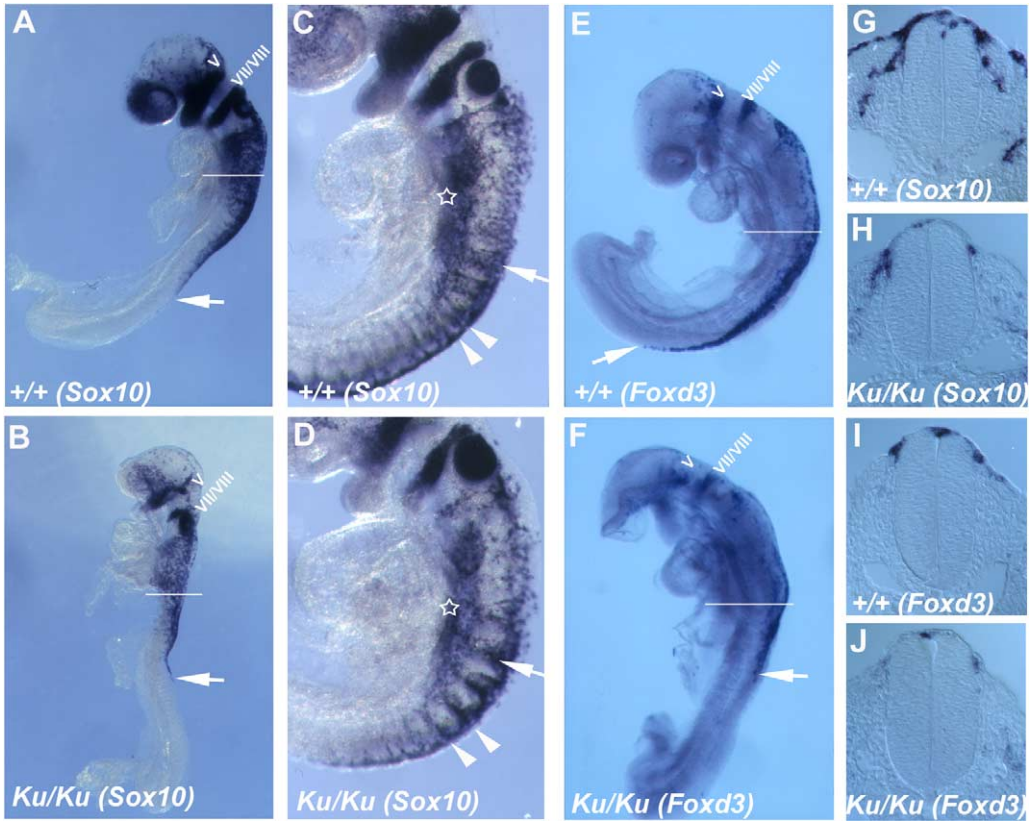

Fig. 4. The neural crest is depleted in Kumba mutants. (A and B) Lateral view of a 13-somite stage wild-type embryo (A) and a 13-somite stage *Zic2*$^{Ku/Ku}$ embryo (B) after in situ hybridisation to *Sox10*. In the mutant embryo neural crest cells form and begin to follow the normal migration pathways. The beginnings of the trigeminal and facial/auditory ganglia can be seen in the wild-type and mutant embryos. The depletion in number of crest cells can be seen in the cranial region, in branchial arches 1 and 2, and in the trunk. The caudal extent of crest cell generation is marked with an arrow. (C and D) Lateral view of the rostral trunk region of a 19-somite stage wild-type embryo (C) and a 19-somite stage *Zic2*$^{Ku/Ku}$ embryo (D) after in situ hybridisation to *Sox10*. In both embryos the neural crest cells migrate in orderly streams through the rostral half of the somites (arrowheads) and in more rostral somites the cells are beginning to condense into the dorsal root ganglia (arrow). Cells at the anterior of the trunk have migrated ventrally to the foregut and sympathetic ganglia region (star). (E and F) Lateral view of a 13-somite stage wild-type embryo (E) and a 13-somite stage *Zic2*$^{Ku/Ku}$ embryo (F) after in situ hybridisation to *Foxd3*. The beginnings of the trigeminal and facial/auditory ganglia can be seen and the caudal limit of neural crest cell generation is marked with an arrow. (G and H) Transverse sections through the trunk of a 13-somite stage wild-type embryo (G) and a 13-somite stage *Zic2*$^{Ku/Ku}$ embryo (H) after in situ hybridisation to *Sox10*, at the level shown in A and B. The number of migrating *Sox10*-positive cells is visibly reduced in the homozygous embryo. (I and J) Transverse sections through the trunk of a 13-somite stage wild-type embryo (I) and a 13-somite stage *Zic2*$^{Ku/Ku}$ embryo (J) after in situ hybridisation to *Foxd3*, at the level shown in E and F. The number of migrating *Foxd3*-positive cells is visibly reduced in the homozygous embryo. V: trigeminal ganglia; VII/VIII: facial/auditory ganglia.

mouse colony has demonstrated cosegregation of the mutation and phenotype over 3521 meioses.

The Kumba heterozygous phenotype is not fully penetrant

The Kumba mouse mutant was originally identified as a line with a variable phenotype that included a ventral spot and/or a curled tail (Nolan et al., 2000). Subsequently a C3H/HeH congenic line carrying the mutation was produced. The congenic strain exhibits two additional heterozygous phenotypes: a small proportion of mice are born with spina bifida while others exhibit a slight kink at the end of the tail (Fig. 3). Although the expected number of heterozygotes are born and survive to weaning, none of the phenotypes are fully penetrant (Table 1). To examine the homozygous phenotype, intercross litters were dissected at different embryonic time points. At 9.5 dpc *Zic2*$^{Ku/Ku}$ embryos can be distinguished from their wild-type littermates based on an open cranial neural tube, delayed posterior neuropore closure, and haemotomas that are most often associated with the forebrain (Fig. 3). At this time point homozygous embryos are recovered at the expected Mendelian frequency; however, when embryos are dissected at 13.5 dpc all of the homozygotes are dead or dying (Table 2).

Neural crest development in Kumba mutants

The ventral spotting associated with the *Zic2*$^{Ku/+}$ mutation suggested that neural crest production, migration, and/or differentiation might be compromised in these mice. To investigate the role of *Zic2* in neural crest development *Zic2*$^{Ku/Ku}$ embryos were examined with a variety of neural

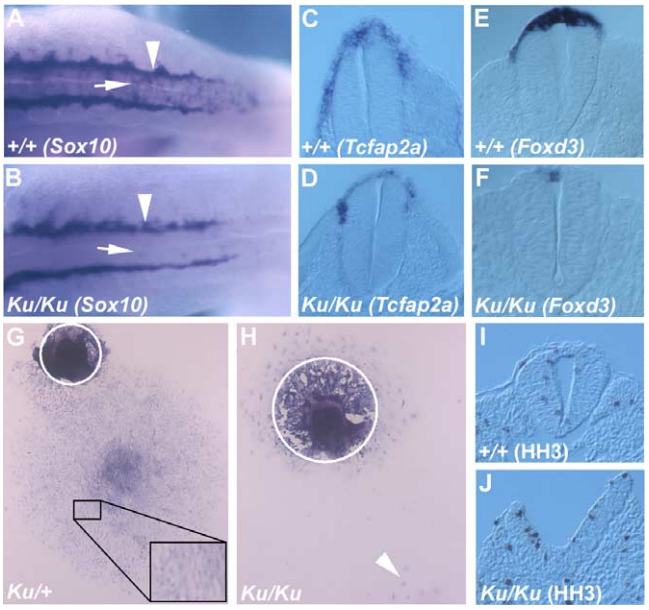

Fig. 5. Neural crest proliferation and induction. (A and B) Dorsal view of an 18-somite wild-type embryo (A) and an 18-somite *Zic2*$^{Ku/Ku}$ embryo (B) after in situ hybridisation to *Sox10*, showing the neural crest. The arrows show the dorsal midline of the neural tube and the arrowheads mark migrating neural crest cells lateral of the neural tube. There are fewer Sox10-positive cells in the mutant neurectoderm. (C and D) Transverse sections through the trunk of an 18-somite stage wild-type embryo (C) and an 18-somite stage *Zic2*$^{Ku/Ku}$ embryo (D) after in situ hybridisation to *Tcfap2a*, at the posterior limit of *Tcfap2a* expression in the mutant and wild-type embryos. (E and F) Sections through the posterior trunk of an 18-somite wild-type (E) and an 18-somite mutant embryo (F) after in situ hybridisation to *Foxd3*, at the posterior limit of *Foxd3* expression in the mutant and wild-type embryos. (G and H) Posterior neural tube explant cultures from an 18-somite *Zic2*$^{Ku/+}$ embryo (G) and an 18-somite *Zic2*$^{Ku/Ku}$ embryo (H) after 60 h of growth. The neural tube tissue is marked by a circle in each picture. The insert in G shows the neural crest cells at the same magnification as in H. The *Zic2*$^{Ku/Ku}$ neural crest cells are capable of migrating a large distance from the neural tissue as shown by the cells marked with an arrowhead. (I and J) Sections through a 20-somite wild-type embryo just anterior to the posterior neuropore (I) and at an equivalent axial level in a 19-somite *Zic2*$^{Ku/Ku}$ embryo (J) after detection of mitotic cells with the anti-phospho-histone H3 antibody. The number of mitotically active cells is unaffected in the mutant.

crest markers. Between 8.5 and 10.5 dpc the HMG box transcription factor *Sox10* is expressed exclusively in the crest-forming region of the neural plate, the migrating crest cells, and the ganglia populated by these cells (Southard-Smith et al., 1998). The winged helix transcription factor *Foxd3* is expressed in newly induced and migrating crest cells (Dottori et al., 2001). Transcription factor AP2 (*Tcfap2a*) is expressed in neural crest cells and their major derivatives (Mitchell et al., 1991). This WMISH analysis revealed two features of crest development in the mutant embryos that were seen with all three markers. First, as can be seen in Fig. 4 at the stages examined there appears to be a reduction in the number of neural crest cells produced both in the cranial region and in the trunk. Second, in all embryos examined the posterior limit of crest was shifted rostrally relative to wild-type, stage-matched controls. The consistency of these features over three different neural crest cell molecular markers makes it highly probable that these differences reflect aberrant neural crest development rather than a specific effect on the expression of each gene. The visible alterations in the distribution of these three markers of early stages of crest development show that *Zic2* acts relatively early in the genetic programme that generates neural crest, rather than in later processes such as neural crest differentiation. The early steps in neural crest development include the establishment of a "progenitor zone" within the neurectoderm at the neural plate border, neural crest cell progenitor induction, progenitor proliferation, and crest migration.

Neural crest migration in Kumba mutants

Of the three molecular markers examined, *Sox10* is the best marker of the early stages of neural crest migration. The WMISH analysis with *Sox10* demonstrated that the general pattern of crest migration was largely unaltered in the mutant embryos, with the main defect appearing to be less migrating cells rather than an aberrant pattern of migration. In the mouse embryo the midbrain and hindbrain crest migrates early, before cranial neural tube closure. At 9.0 dpc (12 somite stage) *Zic2*$^{Ku/Ku}$ embryos contain few midbrain-derived crest cells within the cranial mesenchyme. The first and second branchial arches and cranial ganglia V, VII, and VIII all form in the correct locations but contain visibly fewer cells than in wild-type, stage-matched littermates (Fig. 4A and B, and E and F). Likewise in the trunk region of *Zic2*$^{Ku/Ku}$ embryos the pattern of migration is not markedly different from that of the wild-type embryos. At all stages examined, in the rostral portion of the trunk, neural crest cells were present and distributed in a manner similar to that of wild-type embryos. In 18-somite *Zic2*$^{Ku/Ku}$ embryos it can be seen that the crest cells migrate through the rostral half of the somites, the beginnings of dorsal root ganglia condensations are apparent, and crest cells have migrated to the foregut and future sympathetic ganglia (Fig. 4C and D). However, in all regions of *Sox10* expression it can be seen that there appears to be less *Sox10* expressing cells in *Zic2*$^{Ku/Ku}$ mutants than in their wild-type stage-matched littermates. To determine whether this is due to a decreased number of *Sox10*-positive cells these embryos were sectioned and the number of *Sox10*-expressing, migrating neural crest cells were counted. The counts were carried out in comparable sections from an equivalent axial level (the trunk posterior to the heart) in mutant and wild-type embryos as described in the Materials and methods section. Analysis of the total number of migrating crest cells in the sections demonstrated that *Zic2*$^{Ku/Ku}$ embryos are significantly depleted of *Sox10*-expressing neural crest cells with the mutant embryos containing approximately half of the number of crest cells in wild-type sections (Table 3). The reduction in the number of neural crest cells was found at axial levels where there is no neural tube closure defect

Table 3
The distribution of migrating *Sox10*-positive neural crest cells[a]

Embryo	SE	VL	VM	All migrating cells
13/14 som, $Zic2^{+/+}$	3.33 ± 0.50 (100)	14.42 ± 1.42 (100)	5.71 ± 0.72 (100)	20.13 ± 1.35 (100)
13/14 som, $Zic2^{Ku/Ku}$	0.44 ± 0.18[b] (13)	9.00 ± 0.83[b] (62)	1.94 ± 0.44[b] (34)	11.38 ± 1.04[b] (57)
18 som, $Zic2^{+/+}$	2.74 ± 0.12 (100)	35.70 ± 0.61 (100)	6.57 ± 0.18 (100)	45.00 ± 0.66 (100)
18 som, $Zic2^{Ku/Ku}$	0.13 ± 0.02[b] (5)	16.25 ± 0.36[b] (46)	4.83 ± 0.15 (74)	21.21 ± 0.41[b] (47)

[a] A set of 10–12 representative sections was scored from each mutant or wild-type embryo as described in the materials and methods section. Embryos with 13 or 14 somites (som) ($Zic2^{+/+}$: $n = 24$ observations from 2 embryos; $Zic2^{Ku/Ku}$: $n = 36$ observations from 3 embryos) and embryos with 18 somites ($Zic2^{+/+}$: $n = 23$ observations from 2 embryos; $Zic2^{Ku/Ku}$: $n = 24$ observations from 2 embryos) were scored. Data were pooled within time-point and genotype classes and the mean number of cells per section calculated. Data are shown as the mean ± SEM values. The number in brackets shows the total number of *Sox10*-positive cells as a percentage of the total number of *Sox10*-positive cells in the corresponding wild-type data set.

[b] Number of cells per section is significantly different to the corresponding wild-type data set, $P < 0.05$ (2 tailed t test); SE: subectodermal; VL: ventrolateral; VM: ventromedial.

(see Fig. 4G–J) demonstrating that this phenotype is not secondary to the aberrant neurulation. One straight forward explanation for the decrease seen in the number of migrating cells is that the correct numbers of neural crest cells are initially produced but that a proportion of these subsequently die. However, an examination of mutant embryos using TUNEL analysis did not reveal an increase in cell death in either the crest-forming region of the dorsal neural tube or along the neural tube migration pathways (data not shown).

After the neural crest is formed it begins to migrate away from the neural tube along defined migration pathways. Lineage-tracing experiments have shown that in the mouse the earliest migrating trunk crest follows one of two pathways: subectodermal or ventrolateral. The subectodermal cells will eventually form the pigment-producing melanocytes and the ventrolateral cells will populate ventral crest derivatives including the sympathetic ganglia, the adrenal medulla, and the aortic plexuses. Later, some of the crest will follow a ventromedial pathway and migrate between the somite and the neural tube to contribute to the dorsal root ganglia. Subsequently, migration along the ventrolateral pathway will diminish such that only the ventromedial and subectodermal migration continues (Serbedzija et al., 1990, 1994). The neural crest cell analysis presented in Fig. 4 was carried out during the stage at which crest cells are migrating along each of the three pathways. To determine whether the reduction in neural crest cells was confined to a particular migration route, the same sections used to determine the total number of crest cells were further analysed. In each section the number of cells following the three migration pathways were counted and the data summarised in Table 3. It can be seen that the crest cells are able to migrate along each of the three usual pathways; however, these pathways are differentially affected. The number of cells following either the subectodermal or the ventrolateral pathways are consistently significantly reduced while the ventromedial pathway is only affected in the younger embryos.

Neural crest proliferation in Kumba mutants

The decrease in the number of migrating neural crest cells may reflect an inability to expand the neural crest progenitor pool via proliferation. To examine this possibility the anti-phospho-histone H3 antibody was used to highlight mitotic cells in the dorsal neural tube. Examination of wild-type neural tubes along the trunk region showed that there is a significant increase in the number of mitotic cells at the anterior of the posterior neuropore and in the sections immediately rostral of this region (Table 4). Embryos homozygous for the *Ku* mutation also showed an elevated number of mitotic cells in this region and no difference was observed between the mutant and wild-type embryos in this respect. The number of mitotic cells was also compared in a more rostral region of trunk neurectoderm corresponding to the region where neural crest cells are first observed in the mutant embryos. Again, no difference in the number of cells in mitosis was detected between the mutant embryos and wild-type embryos at this axial level (Table 4 and Fig. 5I and J).

Neural crest formation in Kumba mutants

The initial WMISH analysis with *Sox10, Foxd3,* and *Tcfap2a* showed that when the embryos were viewed in

Table 4
The distribution of mitotically active dorsal neurectoderm cells[a]

Embryo	Caudal sections	Rostral sections
17–20 somite, $Zic2^{+/+}$	4.06 ± 0.23	1.86 ± 0.14[b]
17–20 somite, $Zic2^{Ku/Ku}$	3.53 ± 0.46	1.59 ± 0.15[b]

[a] A set of 10–20 representative sections was scored from each mutant or wild-type embryo as described in the materials and methods section. Embryos with 17–20 somites ($Zic2^{+/+}$: $n = 50$ observations from 3 embryos; $Zic2^{Ku/Ku}$: $n = 30$ observations from 2 embryos) were scored. Data were pooled within time-point and genotype classes and the mean number of cells per section calculated. Data are shown as the mean ± SEM.

[b] The number of cells per section in the rostral data set is significantly different to the corresponding caudal data set, $P < 0.05$ (2 tailed t test).

Table 5
The distribution of premigratory *Foxd3*-positive neural crest cells[a]

Embryo	No. of cells/section
18 somite, *Zic2*$^{+/+}$	8.25 ± 0.90 (100)
18 somite, *Zic2*$^{Ku/Ku}$	2.79 ± 0.66[b] (34)
19 somite, *Zic2*$^{+/+}$	4.67 ± 0.54 (100)
19 somite, *Zic2*$^{Ku/Ku}$	1.58 ± 0.12[b] (34)

[a] A set of 12 representative sections was scored from each mutant or wild-type embryo as described in the materials and methods section. Embryos with 18 somites (*Zic2*$^{+/+}$: $n = 12$ observations from 1 embryo; *Zic2*$^{Ku/Ku}$: $n = 24$ observations from 2 embryos) and embryos with 19 somites (*Zic2*$^{+/+}$: $n = 12$ observations from 1 embryo; *Zic2*$^{Ku/Ku}$: $n = 24$ observations from 2 embryos) were scored. Data were pooled within time-point and genotype classes and the mean number of cells per section calculated. Data are shown as the mean ± SEM. The number in brackets shows the total number of *Foxd3*-positive cells as a percentage of the total number of *Foxd3*-positive cells in the corresponding wild-type data set.

[b] Number of cells per section is significantly different to the corresponding wild-type data set, $P < 0.05$ (2 tailed *t* test).

whole mount there appeared to be a depletion of neural crest cells not only along the migration pathways but also within the neurectoderm and this was confirmed by sectioning (Fig. 5). *Foxd3* is an early and specific marker of premigratory neural crest cells and was therefore judged to be the best marker for a quantitative analysis of the newly formed neural crest cells. For this analysis, serial sections were cut from embryos following WMISH and the number of *Foxd3*-positive cells was counted as described in the Materials and methods section. The number of *Foxd3*-positive cells was initially compared between mutant and wild-type embryos at the most posterior level at which neural crest cells are usually first found. At this level there are no *Foxd3*-positive cells in the mutant embryos demonstrating that neural crest induction is delayed. In the mutant embryos neural crest generation does occur at a more rostral level. The number of *Foxd3*-expressing cells was counted at the most posterior level of crest production in the mutant embryos and compared to the number of cells generated at the posterior limit of crest production in wild-type embryos. It can be seen from Table 5 that in all comparisons the number of *Foxd3*-positive cells is significantly less in the *Zic2*$^{Ku/Ku}$ mutants than in their stage-matched wild-type littermates, reaching only 34% of the wild-type number of cells.

To confirm that the altered *Foxd3* expression pattern results from a delay in the production of neural crest cells in *Zic2*$^{Ku/Ku}$ mutants, a posterior region of neurectoderm was isolated and explanted from both mutant and wild-type stage-matched littermates and cultured on a fibronectin substrate. As shown in Fig. 1 the region of neurectoderm used in these experiments was adjacent to the four posterior-most somites. In the stage of embryos used in these experiments this is the region where the neural crest is just beginning to form, therefore isolating this material will examine whether neural crest-inductive signals have been received by the neurectoderm. In each case a greatly reduced number of cells migrated from the mutant neurectoderm relative to the number that migrated from the wild-type neurectoderm and representative cultures are shown in Fig. 5G and H.

Neural tube patterning in Kumba mutants

A possible explanation for the disruption in neural crest production is that *Zic2* is required to segment the neural plate along the future dorsal-ventral (D-V) axis and in particular to establish the crest-forming neural plate border region. To determine whether the crest phenotype was secondary to a disruption in D-V patterning we examined the expression of several genes that show a restricted pattern in the neural tube. The homeodomain gene *Msx1* is expressed at the margin of the neural plate and in the dorsal part of the closed neural tube (Hill et al., 1989). In *Zic2*$^{Ku/Ku}$ embryos the expression of *Msx1* is unaltered in the closed region of the neural tube, the usual dorsal-ventral limit of expression is maintained, and no difference in the size of the *Msx1*-expressing region was noted (Fig. 6A and B). However *Msx1* expression is lost in regions of the neural tube that are yet to close (Fig. 6G and H). In wild-type embryos, *Msx1* expression does not normally extend throughout the posterior neuropore region suggesting that roofplate signals are required for the maintenance of dorsal *Msx1* expression. It is likely that the effect on *Msx1* expression in *Zic2*$^{Ku/Ku}$ mutants in the posterior region of the embryo is a secondary consequence of the delayed neuropore closure. To further investigate dorsal pattern the expression of *Zic2* was examined. During normal development *Zic2* transcripts are found throughout the entire neural plate at the posterior of the embryo. As the neurectoderm matures *Zic2* expression becomes restricted to the lateral (future dorsal) regions of the neural tube in a process that has been shown to be Shh dependent (Rohr et al., 1999). In *Zic2*$^{Ku/Ku}$ embryos the expression of *Zic2* remains unaltered throughout the entire length of the neural tube and is independent of neuropore closure (Fig. 6I and J). This again demonstrates that dorsal pattern is established normally in the mutant embryos. Additionally, the continued expression of *Zic2* RNA in embryos homozygous for this mutation demonstrates that functioning Zic2 is not required for its own expression. The correct progressive dorsal restriction of *Zic2* transcripts in homozygous embryos implies that the ventral Shh signal is intact. To confirm that ventral pattern is established in *Zic2*$^{Ku/Ku}$ neural tubes we examined the expression of *Shh* at 9.5 dpc. As can be seen from Fig. 6 (E and F), *Shh* is expressed in the floorplate of homozygous 9.5 dpc embryos in the same manner as in wild-type embryos.

Neural crest induction in Kumba mutants

To determine whether the delay in neural crest production resulted from an altered distribution of inducing signals we examined the expression pattern of candidate inducing molecules. Two families of signalling molecules have been shown to be able to induce neural crest in a variety of in

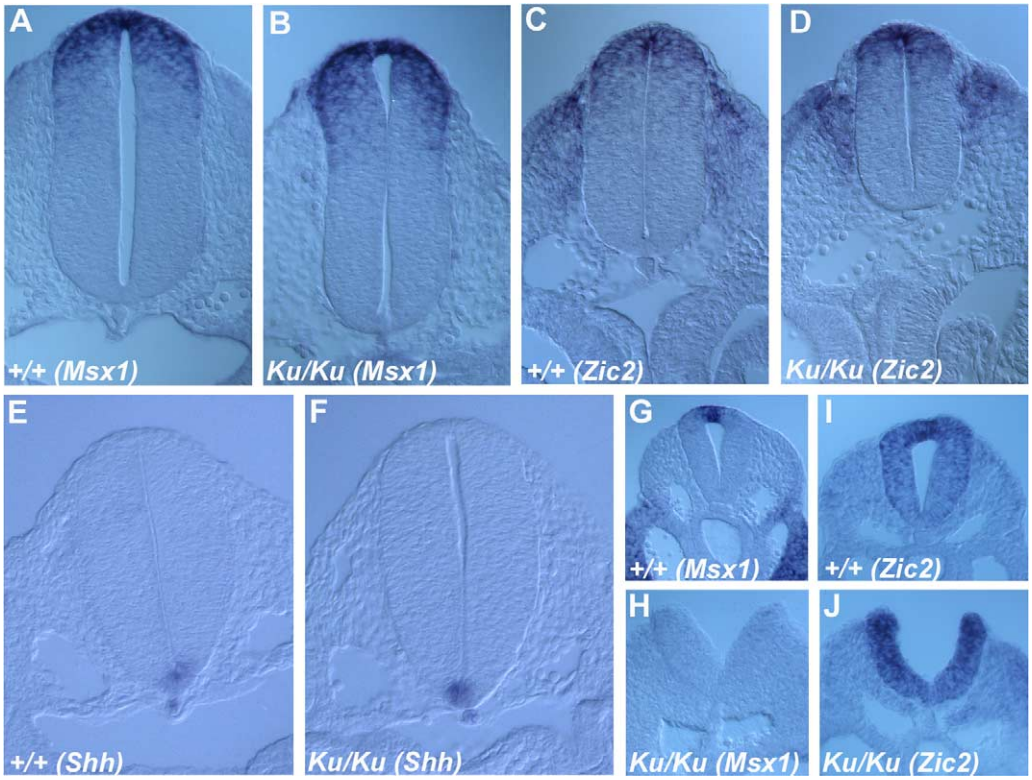

Fig. 6. The Kumba neural tube is correctly patterned. (A and B) A transverse section through the anterior of the trunk of a 14-somite stage wild-type embryo (A) and a 15-somite stage mutant embryo (B) showing that *Msx1* expression remains restricted to the dorsal neural tube. (C and D) Transverse sections through a wild-type 14-somite stage embryo (C) and a 14-somite stage mutant embryo (D) after in situ hybridisation to *Zic2*. In the homozygous embryo *Zic2* is expressed in the same domain as in the wild-type embryo. (E and F) A transverse section through a 16-somite wild-type embryo (E) and a 16-somite stage mutant embryo (F) showing *Shh* expression in the notochord and floorplate. (G and H) Sections through the posterior neural tube of a 14-somite wild-type embryo (G) and a 15-somite mutant embryo (H) after in situ hybridisation to *Msx1*, expression is lost in the mutant in regions where the neural tube has yet to close. (I and J) At the posterior of the embryo *Zic2* is expressed throughout the entire neural plate in a wild-type 14-somite embryo (I) and a 14-somite mutant embryo (J).

vitro and in vivo approaches. In the chick BMP and Wnt molecules are able to induce neural crest from naive ectoderm in explant assays and blocking these signalling pathways disrupts crest formation (for review, see Knecht and Bronner-Fraser, 2002). During neural crest induction in the chick several *BMP*s are expressed in the manner expected of an endogenous inducing molecule, while of the *Wnt* family members *Wnt6* is expressed appropriately (Liem et al., 1995; Schultheiss et al., 1997; Schubert et al., 2002; Garcia-Castro et al., 2002). In the mouse *BMP* genes have been shown to be involved in neural crest production. *BMP7* can induce cranial neural crest in an overexpression assay (Arkell and Beddington, 1997) and mutants lacking both *BMP7* and *BMP5* are depleted in trunk neural crest (Solloway and Robertson, 1999). The function of *Wnt6* in induction of the mouse trunk neural crest has not been investigated to date and the expression pattern of *Wnt6* during the period of crest induction is not well documented (Parr et al., 1993). We therefore first examined *Wnt6* transcript accumulation in the regions of trunk neural crest formation in wild-type mouse embryos. We found that in the mouse, as in the chick, *Wnt6* is expressed in a pan-epidermal manner, consistent with a role in neural crest induction (Fig. 7). We examined the expression pattern of both *Wnt6* and *BMP7* in $Zic2^{Ku/Ku}$ embryos and found no differences in the distribution of transcripts relative to the wild-type expression pattern. As shown in Fig. 7 *BMP7* and *Wnt6* expression remained unaltered, both genes are expressed throughout the surface ectoderm, including that over the neurectoderm. BMP7 expression is also found within the dorsal neurectoderm.

Segmentation in Kumba mutants

The *Drosophila* homologue of the *Zic* genes, *opa*, is involved in segmentation of the body and it is known that in vertebrates the segmenting paraxial mesoderm can influence the development of the neural crest in the overlying neurectoderm. To determine whether a defect in somite formation may be responsible for the neural crest phenotype we examined the expression of the TGFβ antagonist follistatin. Follistatin is expressed in all of the segmented trunk mesoderm (somites) and in the segmented rhombomeres of the hindbrain (Albano et al., 1994). This analysis did not detect any alterations in somite segmentation, but did reveal aberrant hindbrain pattern. In $Zic2^{Ku/Ku}$ embryos rhombomeres (r) 3 and 5 are reduced in size and follistatin expression is

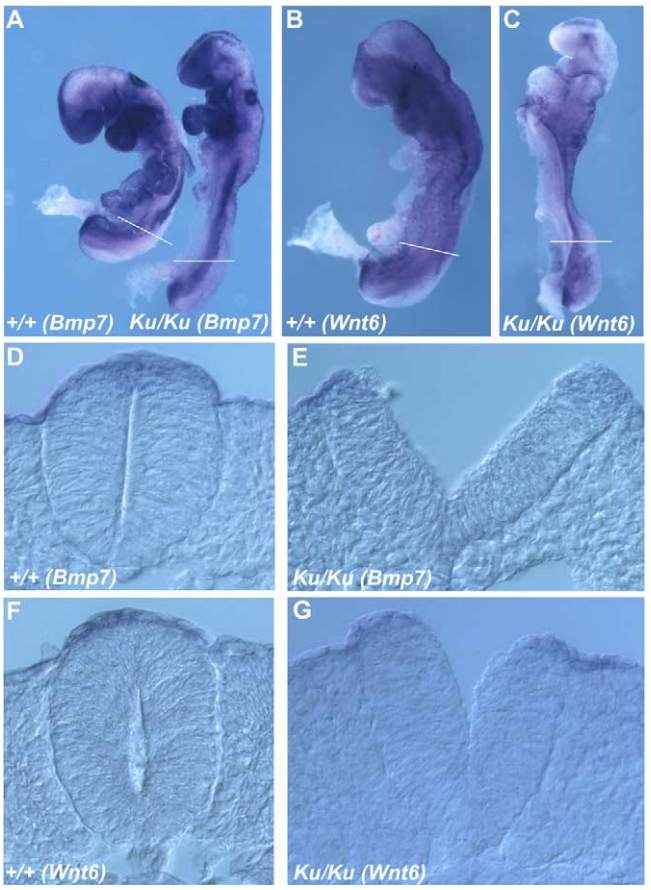

Fig. 7. Expression of *Bmp7* and *Wnt6* is unaltered in Kumba mutants. (A) Lateral view of 13-somite stage wild-type and $Zic2^{Ku/Ku}$ embryos after WMISH to *Bmp7*. (B and C) Lateral view of an 11-somite stage wild-type embryo (B) and a 12-somite stage $Zic2^{Ku/Ku}$ embryo (C) after WMISH to *Wnt6*. (D and E) Transverse sections through the posterior neural tube of a 13-somite stage wild-type (D) and $Zic2^{Ku/Ku}$ (E) embryo after WMISH to *BMP7* at the level shown in A. (F and G) Transverse sections through the posterior neural tube of an 11-somite stage wild-type (F) and 12-somite stage $Zic2^{Ku/Ku}$ (G) embryo after WMISH to *Wnt6* at the levels shown in B and C.

not confined to r2, 4, and 6, but extends throughout r3 and r5 (Fig. 8). To further investigate this we examined the expression of *Krox20 (Egr2)*, a zinc finger transcription factor that is expressed specifically in r3 and r5 (Wilkinson et al., 1989), as well as the expression of the homeobox gene *Hoxa2*, which is upregulated in r3 and r5 due to direct regulation by *Krox20* (Nonchev et al., 1996). In both cases, the temporospatial expression of these genes in the neurectoderm and emerging neural crest was normal, although r3 and r5 were small.

Discussion

The Kumba mutation

A hypomorphic allele of mouse *Zic2* has been generated by gene targeting (Nagai et al., 2000) and this mutant (which is estimated to retain only 20% of *Zic2* transcript in homozygotes) shows a phenotype that is similar to, although milder than, that of the Kumba allele. Mice that are homozygous for the hypomorphic allele are born with spina bifida whereas mice heterozygous for the *Ku* allele exhibit spina bifida at birth. With respect to this and other aspects of the phenotype the Kumba allele causes a more severe effect than a partial loss of function allele, indicating that Kumba is a loss of function mutation. The existence of another allele of *Zic2* establishes that the *Ku* phenotype is caused by the mutation identified here and argues against a second, unidentified mutation underlying the phenotype. This possibility is further excluded by the breeding scheme used to maintain the Kumba colony. Based on the average frequency of ENU mutagenesis (0.001 per locus per gamete) (Hitotsumachi et al., 1985) and the number of genes in the mouse genome (approximately 30,000) (Waterston et al., 2002) we can estimate that the original F1 mouse with the visible phenotype harboured in the order of 30 mutated genes. Theoretically the number of independent mutations carried by the mouse line will decrease by 50% with each backcross, meaning that there is a high probability that mice from backcross generation 5 and beyond will carry only the causative mutation. All of the animals used in this study were from the 10th backcross generation and beyond.

The point mutation in the *Zic2* gene described here changes an invariant amino acid that is known to be essential for the metal binding ability of zinc fingers, and metal binding is required for the structural integrity of zinc finger domains (Michael et al., 1992). Moreover, identical amino acid substitutions have been shown to generate null alleles of at least two other zinc finger proteins; yeast *ADR1* and *Drosophila* Kruppel (*Kr*). In each case the phenotype of mutants with an altered zinc ligand in only one zinc finger domain corresponds to that generated by gene deletion (Blumberg et al., 1987; Redemann et al., 1988). In the case of the ADR1 protein 19 independently generated, phenotype-producing mutations were studied. All 12 mutations that caused a substitution at a single zinc ligand generated null alleles. This demonstrates that the disruption of metal binding within one zinc finger is sufficient to completely abolish the biological function of the entire zinc finger domain. These data predict that the Kumba mutation will generate a null allele, providing zinc finger-independent activities do not reside outside of the *Zic2* zinc finger domain. To date, when tested, the zinc finger domain of the *Zic* genes has been shown to be required for the identified biochemical functions (Koyabu et al., 2001). Many examples exist of mutations within zinc finger domains that generate dominant negative molecules. However, such mutations have not been associated with alteration of the zinc coordinating residues. Instead these types of mutations affect DNA binding, protein binding, or protein modification residues (Nichols et al., 2000; Person et al., 2003). In the absence of further genetic or biochemical data we cannot exclude the possibility that *Zic2* loss of function is due to

the production of a competitive molecule. The existence of this point mutation provides us with a tool to extend our understanding of the biochemical function of the *Zic* genes.

Neural crest cell number

In the mouse the emigration of the cranial neural crest is completed before neural tube closure (Serbedzija et al., 1992) and emigration of the trunk neural crest begins before the first closure of the trunk neural tube. Furthermore, mouse mutants that have a complete failure of neural tube closure do not have defects in neural crest production (Henderson et al., 2001). Thus, in the mouse, neural crest production and emigration is not dependent upon neural tube closure. The neural crest defects in *Ku* mutants are observed at all axial levels even though closure defects are only found in the cranial neural tube and at the posterior neuropore. The regionalised closure defects cannot provide an explanation for the global neural crest defect and *Zic2* must play a primary role in crest production.

The data presented here provide the first evidence that *Zic2* is involved in mammalian neural crest development. One finding from this study is that embryos lacking Zic2 produce a decreased number of neural crest cells. There is a depletion not only of migrating neural crest cells but also in the number of premigratory cells produced within the neural ectoderm. The finding that the number of cells is decreased from the earliest stages of neural crest formation means that the primary defect is not in migration or in maintenance or survival of the neural crest cells. Defects in maintenance or survival are also excluded by the fact that the occurrence of cell death is not increased in the mutants. Consistent with the proposal that *Zic2* acts in an early aspect of neural crest formation, *Zic2* is expressed throughout the dorsal region of the neural tube within the neural crest progenitor zone. When *Zic2* is overexpressed in *Xenopus* embryos ectopic neural crest is produced along with anterior neural markers and it is proposed that *Zic2* may function to establish the neural plate border region. A decrease in the size of this region may be expected to lead to a decrease in the number of neural crest cells that are produced. However, our understanding of this border region is based largely upon the availability of molecular markers that are expressed at the lateral margin (and later at the dorsal midline) of the neurectoderm, such as *Msx1* and *Zic2*. Our analysis of these markers did not detect a decrease in the size of the dorsal crest-forming region implying that *Zic2* is required for a later step in neural crest development.

A further possibility is that the reduction in the number of neural crest cells occurs because in $Zic2^{Ku/Ku}$ mutants the normal number of crest progenitors is produced, but this pool is not expanded appropriately. However, we found no evidence that the proliferative behaviour of the dorsal neurectoderm is altered in response to mutation of *Zic2*. This finding, in combination with the altered timing of neural crest production (see below), could explain a decrease in the number of neural crest cells. The combined results of the neural crest cell experiments presented here are represented in Fig. 9. We found that in wild-type embryos there is a significant increase in the occurrence of mitotic cells at the anterior of the posterior neuropore and in the sections immediately rostral of this region. In wild-type embryos this region overlaps with the site of the first expression of *Foxd3*. In the mutant embryos there is no significant change in the number of mitotic cells within this region of the neurectoderm. Additionally, in the region where neural crest cells are first seen in the mutant embryos (as marked by *Foxd3* expression), there is no significant increase in the number of proliferating cells in the dorsal neural tube. It appears that in the mutant embryos neural crest is first produced in a region of the neural tube that has a low rate of dorsal proliferation relative to the usual site of induction. It is possible that this is the cause of the decrease in the number of neural crest cells produced in the mutants. In this case *Zic2* would not play a direct role in determining the number of neural crest cells, and the depletion in cells would be a secondary consequence of the delay in neural crest production.

Neural crest induction

Our data show that as the result of a mutation in *Zic2* the expression of *Foxd3* in the dorsal neural tube is considerably delayed. This appears to represent a delay in neural crest production since *Foxd3* is an early, specific marker of neural crest cells and in the mouse *Foxd3* appears to be expressed in the precursors of all neural crest lineages (Dottori et al., 2001). Additionally, when neurectoderm that should already have received induction signals is explanted from mutant embryos very few neural crest cells are formed. TUNEL experiments confirm that the lack of premigratory neural crest cells in this region of the embryo is not due to cell death; likewise cell death was not seen in the neural crest cell cultures. As described above, the number of proliferating cells in the neural tube remains unaltered in $Zic2^{Ku/Ku}$ embryos demonstrating that *Zic2* does not function at the stage of progenitor proliferation. It appears that the primary defect in the mutant embryos is a delay in the conversion of cells within the dorsal progenitor zone into committed neural crest progenitor cells. This process occurs within the dorsal neurectoderm in response to inductive signals. The current experiments suggest that the delay is not due to *Zic2* having a direct role in the transcriptional control of candidate inducing molecules. Both *BMP7* and *Wnt6* are expressed appropriately in $Zic2^{Ku/Ku}$ embryos. This argues that *Zic2* acts downstream of the inducing signals and since *Zic2* is a transcription factor expressed within the neurectoderm it is most likely involved in the interpretation of the neural crest-inducing signals.

It is not clear why mutation of *Zic2* delays (rather than prohibits) neural crest progenitor production. One possibility is that other family members can compensate for the

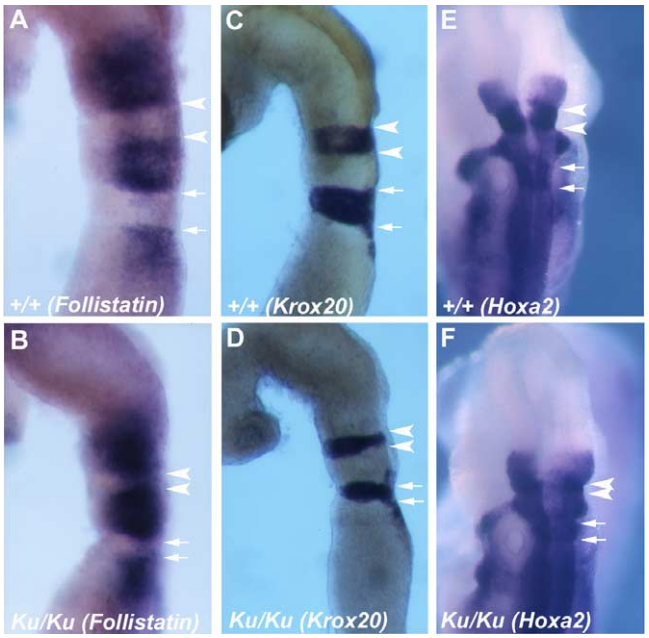

Fig. 8. Aberrant hindbrain pattern in the Kumba mutant. In all pictures the extent of rhombomere 3 is marked with arrowheads and the limit of rhombomere 5 is marked with arrows. (A and B) Lateral view of the hindbrain of a 16-somite stage wild-type embryo (A) and 17-somite stage *Zic2*$^{Ku/Ku}$ embryo (B) after in situ hybridisation to follistatin. In the mutant embryo rhombomeres 3 and 5 are smaller than in the wild-type embryo and follistatin expression is not repressed. (C and D) Lateral view of the hindbrain of a 16-somite stage wild-type embryo (C) and 16-somite stage *Zic2*$^{Ku/Ku}$ embryo (D) after in situ hybridisation to *Krox20 (Egr2)*. *Krox20* is expressed normally in rhombomeres 3 and 5 of the mutant. (E and F) Dorsal view of the hindbrain of a 16-somite stage wild-type (E) and a 17-somite stage *Zic2*$^{Ku/Ku}$ embryo (F) after in situ hybridisation to *Hoxa2* demonstrating that *Hoxa2* is expressed correctly in the hindbrain and in the neural crest that emerges from rhombomeres 4 and 6.

normal function of Zic2. Three other closely related genes (*Zic1*, *Zic3*, and *Opr*) are all expressed within the dorsal neurectoderm at the appropriate stage to act in crest specification and all of these genes can induce ectopic neural crest in *Xenopus* overexpression assays. It is possible that in the mutant embryos these genes do compensate for *Zic2* but that an altered efficiency of these molecules, or the time taken to establish the compensation mechanism, accounts for the delay. Mutation of other *Zic* genes also leads to neural crest and hindbrain phenotypes (Elms, P., Arkell, R., unpublished data) supporting the notion that partial redundancy is responsible for the relatively mild phenotype of the Kumba mutant. Experiments that ablate multiple *Zic* genes are required to determine whether the family members cooperate during crest induction.

A second possibility is that the delay represents a requirement for *Zic2* in the interpretation of only some neural crest-inducing signals. Although it is not known exactly when the signals that direct crest induction occur and which molecules induce neural crest in the mouse, recently it has been suggested that neural crest induction involves two, temporally separated signals (Knecht and Bronner-Fraser, 2002). Selleck et al. (1998) have demonstrated that in the chick BMP antagonists can only inhibit crest production when added to neural tissue around the time of neural tube closure. This implies that an earlier, BMP-independent signal is required for initial crest induction and Selleck et al. (1998) propose that this first signal is generated at least as early as the level of the open neural plate. The most likely candidate for the early signal is Wnt6 (Garcia-Castro et al., 2002). Our data are consistent with a model in which *Zic2* responds to the early signal to generate neural crest cells. In this scenario the *Zic2*$^{Ku/Ku}$ neurectoderm would respond to the later signal, resulting in an apparent delay in the timing of induction. This model is also consistent with the finding that the earliest migrating crest (the subectodermal and ventral-lateral crest) is more severely depleted in the mutants.

Zic2 and hindbrain patterning

The *Drosophila opa* gene is a pair rule gene and is required for segmentation of the embryo. Despite the fact

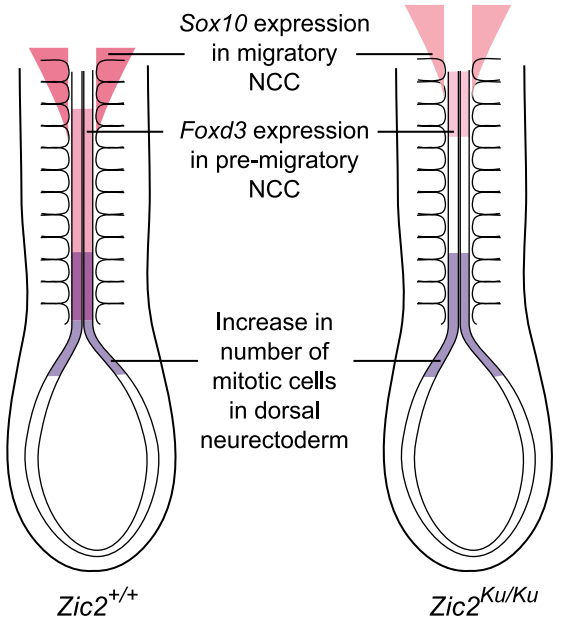

Fig. 9. Neural crest cell development in Kumba mutants. The results of neural crest analysis obtained from separate embryos are represented on a diagram of a single embryo. In wild-type embryos with approximately 18 somites a region of increased mitotic activity was found at the posterior of the embryo in the region of the closing neural plate (light purple). This region overlaps the region of *Foxd3* expression in premigratory cells (pink, with the overlap shown in purple). *Foxd3* expression is seen for several somite lengths before the appearance of *Sox10*-expressing migratory cells (dark pink). In mutant embryos at the same stage, the region of increased mitotic activity is unaltered, but there is no overlap with the region of *Foxd3*-expressing cells (pink). The region of *Sox10*-expressing cells remains relatively unaltered (dark pink) and is almost coincident with the first expression of *Foxd3*. In the mutant embryos there are less *Foxd3* and *Sox10*-positive cells than in the corresponding wild-type region (indicated by lighter shading).

that *Zic* genes are the vertebrate homologues of *opa*, until now, no role for the *Zic* genes in the development of the segmented structures of vertebrates has been demonstrated. We show here that *Zic2* contributes to the development of the transient segmented structures that form within the hindbrain, called rhombomeres. When *Zic2* is mutated, segmentation occurs; however, rhombomeres 3 and 5 are smaller than is usual and follistatin expression in these rhombomeres is not repressed. In these morphological and molecular respects Kumba phenocopies embryos that are null for the C2H2 zinc finger transcription factor *Krox20* (Schneider-Maunoury et al., 1993; Seitanidou et al., 1997). However, *Krox20* is still expressed in r3 and r5 demonstrating that *Zic2* is not required for *Krox20* expression. Furthermore, *Hoxa2* expression is normal in $Zic2^{Ku/Ku}$ embryos. Since *Hoxa2* is upregulated in r3 and r5 due to direct regulation by *Krox20* (Nonchev et al., 1996) this demonstrates that this transcriptional activation property of *Krox20* remains unaltered in *Zic2* mutants. These data are consistent with at least two possibilities. First, *Zic2* and *Krox20* may act independently of one another to mediate the r3 and r5 repression of follistatin. In this case there would be no direct relationship or functional association between *Zic2* and *Krox20*. Second, *Zic2* and *Krox20* may cooperate to regulate follistatin expression. It is already known that *Krox20* is required for the transcriptional repression of some genes and for the transcriptional activation of others. It has been proposed that to act as either a repressor or an activator *Krox20* may interact with distinct cofactors (Seitanidou et al., 1997). If *Zic2* were a cofactor that enabled *Krox20* to act as a repressor then the *Krox20*-mediated upregulation of *Hoxa2* in r3 and r5 would be expected to proceed as normal in *Zic2* mutants. The current experiments do not distinguish between these or other possibilities.

In conclusion the data presented here demonstrate that *Zic2* plays a variety of roles during early neural development. *Zic2* is involved in the generation of the mammalian neural crest. Mutation of *Zic2* generates embryos in which the neural plate is segmented into the correct D-V domains and the neurectoderm proliferates normally yet an insufficient amount of neural crest is generated, and crest production is substantially delayed. It is possible that *Zic2* is required for the interpretation of the signals that induce some of the cells in the neural plate border region to adopt a crest fate. Additionally, *Zic2*, although not required for the initial determination of rhombomeres 3 and 5, does play an important role in the further establishment or maintenance of hindbrain pattern. This work also demonstrates the value of the mouse mutant resources that have been generated through a variety of random mutagenesis screens. Although the only large-scale screens to date have concentrated on the recovery of dominant alleles, a proportion of these mutations will, like Kumba, act in a semidominant manner and have the potential to enhance our knowledge of the mechanisms of embryonic development.

Acknowledgments

We thank I. Mason, I. McGonnell, and V. Wilson for critical reading of the manuscript, T. Hacker for histological processing of specimens, K. Glover for photography of mice, and Z. Tymowska-Lalanne for processing of ABI gels.

References

Albano, R.M., Arkell, R., Beddington, R.S.P., Smith, J.C., 1994. Expression of inhibin subunits and follistatin during postimplantation mouse development: decidual expression of activin and expression of follistatin in primitive streak, somites and hindbrain. Development 120, 803–813.

Arkell, R., Beddington, R.S., 1997. BMP-7 influences pattern and growth of the developing hindbrain of mouse embryos. Development 124, 1–12.

Arkell, R.M., Cadman, M., Marsland, T., Southwell, A., Thaung, C., Davies, J.R., Clay, T., Beechey, C.V., Evans, E.P., Strivens, M.A., Brown, S.D., Denny, P., 2001. Genetic, physical, and phenotypic characterization of the Del(13)Svea36H mouse. Mamm. Genome 12, 687–694.

Aruga, J., Minowa, O., Yaginuma, H., Kuno, J., Nagai, T., Noda, T., Mikoshiba, K., 1998. Mouse Zic1 is involved in cerebellar development. J. Neurosci. 18, 284–293.

Aruga, J., Nagai, T., Tokuyama, T., Hayashizaki, Y., Okazaki, Y., Chapman, V.M., Mikoshiba, K., 1996a. The mouse zic gene family. Homologues of the Drosophila pair-rule gene odd-paired. J. Biol. Chem. 271, 1043–1047.

Aruga, J., Yokota, N., Hashimoto, M., Furuichi, T., Fukuda, M., Mikoshiba, K., 1994. A novel zinc finger protein, zic, is involved in neurogenesis, especially in the cell lineage of cerebellar granule cells. J. Neurochem. 63, 1880–1890.

Aruga, J., Yozu, A., Hayashizaki, Y., Okazaki, Y., Chapman, V.M., Mikoshiba, K., 1996b. Identification and characterization of Zic4, a new member of the mouse Zic gene family. Gene 172, 291–294.

Aybar, M.J., Mayor, R., 2002. Early induction of neural crest cells: lessons learned from frog, fish and chick. Curr. Opin. Genet. Dev. 12, 452–458.

Benedyk, M.J., Mullen, J.R., DiNardo, S., 1994. Odd-paired: a zinc finger pair-rule protein required for the timely activation of engrailed and wingless in Drosophila embryos. Genes Dev. 8, 105–117.

Blumberg, H., Eisen, A., Sledziewski, A., Bader, D., Young, E.T., 1987. Two zinc fingers of a yeast regulatory protein shown by genetic evidence to be essential for its function. Nature 328, 443–445.

Brewster, R., Lee, J., Ruiz i Altaba, A., 1998. Gli/Zic factors pattern the neural plate by defining domains of cell differentiation. Nature 393, 579–583.

Carrel, T., Purandare, S.M., Harrison, W., Elder, F., Fox, T., Casey, B., Herman, G.E., 2000. The X-linked mouse mutation Bent tail is associated with a deletion of the Zic3 locus. Hum. Mol. Genet. 9, 1937–1942.

Chan, W.Y., Tam, P.P.L., 1988. A morphological and experimental study of the mesencephalic neural crest cells in the mouse embryo using wheat germ agglutinin-gold conjugate as the cell marker. Development 102, 427–442.

Denny, P., Brown, S.D.M., 2000. Mapping genomes, in: Jackson, I.J., Abbot, C.M. (Eds.), Mouse Genetics and Transgenics, O.U.P, Oxford, pp. 121–141.

Dottori, M., Gross, M.K., Labosky, P., Goulding, M., 2001. The winged-helix transcription factor Foxd3 suppresses interneuron differentiation and promotes neural crest cell fate. Development 128, 4127–4138.

Dunn, L.C., 1920. Types of white spotting in mice. Am. Naturalist 54, 465–495.

Echelard, Y., Epstein, D.J., St-Jacques, B., Shen, L., Mohler, J., McMahon, J.A., McMahon, A.P., 1993. Sonic hedgehog, a member of a family of putative signaling molecules, is implicated in the regulation of CNS polarity. Cell 75, 1417–1430.

Furushima, K., Murata, T., Matsuo, I., Aizawa, S., 2000. A new murine zinc finger gene, *Opr*. Mech. Dev. 98, 161–164.

Garcia-Castro, M.I., Marcelle, C., Bronner-Fraser, M., 2002. Ectodermal Wnt function as a neural crest inducer. Science 297, 848–851.

Gruneberg, H., Truslove, G.M., 1960. Two closely linked genes in the mouse. Genet. Res. 1, 69–90.

Henderson, D.J., Conway, S.J., Greene, N.D., Gerrelli, D., Murdoch, J.N., Anderson, R.H., Copp, A.J., 2001. Cardiovascular defects associated with abnormalities in midline development in the Loop-tail mouse mutant. Circ. Res. 89, 6–12.

Hertwig, P., 1942. Neue Mutationen und Koppelungsgruppen bei der Hausmaus. Z. Indukt. Abstamm. Vererbungs1. 80, 220–246.

Hill, R.E., Jones, P.F., Rees, A.R., Sime, C.M., Justice, M.J., Copeland, N.G., Jenkins, N.A., Graham, E., Davidson, D.R., 1989. A new family of mouse homeo box-containing genes: molecular structure, chromosomal location and developmental expression of Hox-7.1. Genes Dev. 3, 26–37.

Hitotsumachi, S., Carpenter, D.A., Russell, W.L., 1985. Dose-repetition increases the mutagenic effectiveness of N-ethyl-N-nitrosourea in mouse spermatogonia. Proc. Natl. Acad. Sci. USA 82, 6619–6621.

Hrabe de Angelis, M.H., Flaswinkel, H., Fuchs, H., Rathkolb, B., Soewarto, D., Marschall, S., Heffner, S., Pargent, W., Wuensch, K., Jung, M., Reis, A., Richter, T., Alessandrini, F., Jakob, T., Fuchs, E., Kolb, H., Kremmer, E., Schaeble, K., Rollinski, B., Roscher, A., Peters, C., Meitinger, T., Strom, T., Steckler, T., Holsboer, F., Klopstock, T., Gekeler, F., Schindewolf, C., Jung, T., Avraham, K., Behrendt, H., Ring, J., Zimmer, A., Schughart, K., Pfeffer, K., Wolf, E., Balling, R., 2000. Genome-wide, large-scale production of mutant mice by ENU mutagenesis. Nat. Genet. 25, 444–447.

Justice, M.J., Noveroske, J.K., Weber, J.S., Zheng, B., Bradley, A., 1999. Mouse ENU mutagenesis. Hum. Mol. Genet. 8, 1955–1963.

Kaufman, M.H., Bard, J.B.L., 1999. The Anatomical Basis of Mouse Development. Academic Press, London.

Klootwijk, R., Franke, B., van der Zee, C.E., de Boer, R.T., Wilms, W., Hol, F.A., Mariman, E.C., 2000. A deletion encompassing Zic3 in bent tail, a mouse model for X-linked neural tube defects. Hum. Mol. Genet. 9, 1615–1622.

Knecht, A.K., Bronner-Fraser, M., 2002. Induction of the neural crest: a multigene process. Nat. Rev. Genet. 3, 453–461.

Koyabu, Y., Nakata, K., Mizugishi, K., Aruga, J., Mikoshiba, K., 2001. Physical and functional interactions between Zic and Gli proteins. J. Biol. Chem. 276, 6889–6892.

Lane, P.W., 1982. Dominant megacolon (Dom). Mouse News Lett. 66, 66.

Le Douarin, N.M., Kalcheim, C., 1999. The Neural Crest. Cambridge University Press, Cambridge, UK.

Lennon, G., Auffray, C., Polymeropoulos, M., Soares, M.B., 1996. The I.M.A.G.E. Consortium: an integrated molecular analysis of genomes and their expression. Genomics 33, 151–152.

Liem Jr, K.F., Tremml, G., Roelink, H., Jessell, T.M., 1995. Dorsal differentiation of neural plate cells induced by BMP-mediated signals from epidermal ectoderm. Cell 82, 969–979.

Little, C.C., Cloudman, A.M., 1937. The occurrence of a dominant spotting mutation in the house mouse. Proc. Natl. Acad. Sci. USA 23, 535–537.

Michael, S.F., Kilfoil, V.J., Schmidt, M.H., Amann, B.T., Berg, J.M., 1992. Metal binding and folding properties of a minimalist Cys2His2 zinc finger peptide. Proc. Natl. Acad. Sci. USA 89, 4796–4800.

Miller, J., McLachlan, A.D., Klug, A., 1985. Repetitive zinc-binding domains in the protein transcription factor IIIA from Xenopus oocytes. EMBO J. 4, 1609–1614.

Mitchell, P.J., Timmons, P.M., Hébert, J.M., Rigby, P.W.J., Tjian, R., 1991. Transcription factor AP-2 is expressed in neural crest cell lineages during mouse embryogenesis. Genes Dev. 5, 105–119.

Mizuseki, K., Kishi, M., Matsui, M., Nakanishi, S., Sasai, Y., 1998. Xenopus Zic-related-1 and Sox-2, two factors induced by chordin, have distinct activities in the initiation of neural induction. Development 125, 579–587.

Nagai, T., Aruga, J., Minowa, O., Sugimoto, T., Ohno, Y., Noda, T., Mikoshiba, K., 2000. Zic2 regulates the kinetics of neurulation. Proc. Natl. Acad. Sci. USA 97, 1618–1623.

Nagai, T., Aruga, J., Takada, S., Gunther, T., Sporle, R., Schughart, K., Mikoshiba, K., 1997. The expression of the mouse Zic1, Zic2, and Zic3 gene suggests an essential role for Zic genes in body pattern formation. Dev. Biol. 182, 299–313.

Nakata, K., Koyabu, Y., Aruga, J., Mikoshiba, K., 2000. A novel member of the Xenopus Zic family, Zic5, mediates neural crest development. Mech. Dev. 99, 83–91.

Nakata, K., Nagai, T., Aruga, J., Mikoshiba, K., 1997. Xenopus Zic3, a primary regulator both in neural and neural crest development. Proc. Natl. Acad. Sci. USA 94, 11980–11985.

Nichols, K.E., Crispino, J.D., Poncz, M., White, J.G., Orkin, S.H., Maris, J.M., Weiss, M.J., 2000. Familial dyserythropoietic anaemia and thrombocytopenia due to an inherited mutation in GATA1. Nat. Genet. 24, 266–270.

Nolan, P.M., Peters, J., Strivens, M., Rogers, D., Hagan, J., Spurr, N., Gray, I.C., Vizor, L., Brooker, D., Whitehill, E., Washbourne, R., Hough, T., Greenaway, S., Hewitt, M., Liu, X., McCormack, S., Pickford, K., Selley, R., Wells, C., Tymowska-Lalanne, Z., Roby, P., Glenister, P., Thornton, C., Thaung, C., Stevenson, J.A., Arkell, R., Mburu, P., Hardisty, R., Kiernan, A., Erven, A., Steel, K.P., Voegeling, S., Guenet, J.L., Nickols, C., Sadri, R., Nasse, M., Isaacs, A., Davies, K., Browne, M., Fisher, E.M., Martin, J., Rastan, S., Brown, S.D., Hunter, J., 2000. A systematic, genome-wide, phenotype-driven mutagenesis programme for gene function studies in the mouse. Nat. Genet. 25, 440–443.

Nonchev, S., Vesque, C., Maconochie, M., Seitanidou, T., Ariza-McNaughton, L., Frain, M., Marshall, H., Sham, M.H., Krumlauf, R., Charnay, P., 1996. Segmental expression of Hoxa-2 in the hindbrain is directly regulated by Krox-20. Development 122, 543–554.

Parr, B.A., Shea, M.J., Vassileva, G., McMahon, A.P., 1993. Mouse Wnt genes exhibit discrete domains of expression in the early embryonic CNS and limb buds. Development 119, 247–261.

Person, R.E., Li, F.Q., Duan, Z., Benson, K.F., Wechsler, J., Papadaki, H.A., Eliopoulos, G., Kaufman, C., Bertolone, S.J., Nakamoto, B., Papayannopoulou, T., Grimes, H.L., Horwitz, M., 2003. Mutations in proto-oncogene GFI1 cause human neutropenia and target ELA2. Nat. Genet. 34, 308–312.

Phillips, R.J.S., 1959. New mutants, provisional symbol ls (lethal spotting); my^{1}; and agouti-umbrous a^{u}. Mouse News Lett. 2, 39.

Purandare, S.M., Ware, S.M., Kwan, K.M., Gebbia, M., Bassi, M.T., Deng, J.M., Vogel, H., Behringer, R.R., Belmont, J.W., Casey, B., 2002. A complex syndrome of left-right axis, central nervous system and axial skeleton defects in Zic3 mutant mice. Development 129, 2293–2302.

Redemann, N., Gaul, U., Jackle, H., 1988. Disruption of a putative Cys-zinc interaction eliminates the biological activity of the Kruppel finger protein. Nature 332, 90–92.

Rohr, K.B., Schulte-Merker, S., Tautz, D., 1999. Zebrafish zic1 expression in brain and somites is affected by BMP and hedgehog signalling. Mech. Dev. 85, 147–159.

Rosen, B., Beddington, R.S.P., 1993. Whole-mount in situ hybridization in the mouse embryo: gene expression in three dimensions. Trends Genet. 9, 162–167.

Russell, W.L., 1947. Splotch, a new mutation in the house mouse Mus musculus. Genetics 32, 107.

Schneider-Maunoury, S., Topilko, P., Seitandou, T., Levi, G., Cohen, T.M., Pournin, S., Babinet, C., Charnay, P., 1993. Disruption of

Krox-20 results in alteration of rhombomeres 3 and 5 in the developing hindbrain. Cell 75, 1199–1214.

Schubert, F.R., Mootoosamy, R.C., Walters, E.H., Graham, A., Tumiotto, L., Munsterberg, A.E., Lumsden, A., Dietrich, S., 2002. Wnt6 marks sites of epithelial transformations in the chick embryo. Mech. Dev. 114, 143–148.

Schultheiss, T.M., Burch, J.B., Lassar, A.B., 1997. A role for bone morphogenetic proteins in the induction of cardiac myogenesis. Genes Dev. 11, 451–462.

Seitanidou, T., Schneider-Maunoury, S., Desmarquet, C., Wilkinson, D.G., Charnay, P., 1997. Krox-20 is a key regulator of rhombomere-specific gene expression in the developing hindbrain. Mech. Dev. 65, 31–42.

Selleck, M.A., Garcia-Castro, M.I., Artinger, K.B., Bronner-Fraser, M., 1998. Effects of Shh and Noggin on neural crest formation demonstrate that BMP is required in the neural tube but not ectoderm. Development 125, 4919–4930.

Serbedzija, G.N., Bronner-Fraser, M., Fraser, S.E., 1992. Vital dye analysis of cranial neural crest cell migration in the mouse embryo. Development 116, 297–307.

Serbedzija, G.N., Bronner-Fraser, M., Fraser, S.E., 1994. Developmental potential of trunk neural crest cells in the mouse. Development 120, 1709–1718.

Serbedzija, G.N., Fraser, S.E., Bronner-Fraser, M., 1990. Pathways of trunk neural crest cell migration in the mouse embryo as revealed by vital dye labelling. Development 108, 605–612.

Solloway, M.J., Robertson, E.J., 1999. Early embryonic lethality in Bmp5; Bmp7 double mutant mice suggests functional redundancy within the 60A subgroup. Development 126, 1753–1768.

Southard-Smith, E.M., Kos, L., Pavan, W.J., 1998. Sox10 mutation disrupts neural crest development in Dom Hirschsprung mouse model. Nat. Genet. 18, 60–64.

Waterston, R.H., Lindblad-Toh, K., Birney, E., Rogers, J., Abril, J.F., Agarwal, P., Agarwala, R., Ainscough, R., Alexandersson, M., An, P., Antonarakis, S.E., Attwood, J., Baertsch, R., Bailey, J., Barlow, K., Beck, S., Berry, E., Birren, B., Bloom, T., Bork, P., Botcherby, M., Bray, N., Brent, M.R., Brown, D.G., Brown, S.D., Bult, C., Burton, J., Butler, J., Campbell, R.D., Carninci, P., Cawley, S., Chiaromonte, F., Chinwalla, A.T., Church, D.M., Clamp, M., Clee, C., Collins, F.S., Cook, L.L., Copley, R.R., Coulson, A., Couronne, O., Cuff, J., Curwen, V., Cutts, T., Daly, M., David, R., Davies, J., Delehaunty, K.D., Deri, J., Dermitzakis, E.T., Dewey, C., Dickens, N.J., Diekhans, M., Dodge, S., Dubchak, I., Dunn, D.M., Eddy, S.R., Elnitski, L., Emes, R.D., Eswara, P., Eyras, E., Felsenfeld, A., Fewell, G.A., Flicek, P., Foley, K., Frankel, W.N., Fulton, L.A., Fulton, R.S., Furey, T.S., Gage, D., Gibbs, R.A., Glusman, G., Gnerre, S., Goldman, N., Goodstadt, L., Grafham, D., Graves, T.A., Green, E.D., Gregory, S., Guigo, R., Guyer, M., Hardison, R.C., Haussler, D., Hayashizaki, Y., Hillier, L.W., Hinrichs, A., Hlavina, W., Holzer, T., Hsu, F., Hua, A., Hubbard, T., Hunt, A., Jackson, I., Jaffe, D.B., Johnson, L.S., Jones, M., Jones, T.A., Joy, A., Kamal, M., Karlsson, E.K., et al., 2002. Initial sequencing and comparative analysis of the mouse genome. Nature 420, 520–562.

Wilkinson, D.G., 1992. Whole mount in situ hybridisation of vertebrate embryos, in: Wilkinson, D.G. (Ed.), In Situ Hybridisation, IRL Press, Oxford, pp. 75–83.

Wilkinson, D.G., Bhatt, S., Chavier, P., Bravo, R., Charnay, P., 1989. Segment-specific expression of a zinc-finger gene in the developing nervous system of the mouse. Nature 337, 461–464.